ELSEVIER

Palaeogeography, Palaeoclimatology, Palaeoecology 185 (2002) 339–354

PALAEO

www.elsevier.com/locate/palaeo

Differential response of vegetation to postglacial climate in the Lower Salmon River Canyon, Idaho

Loren G. Davis [a,*], Karlis Muehlenbachs [b], Charles E. Schweger [a], Nathaniel W. Rutter [b]

[a] *Department of Anthropology, University of Alberta, 13-15 Tory Bldg., Edmonton, AB, Canada T6G 2H4*

[b] *Department of Earth and Atmospheric Sciences, University of Alberta, EAS Bldg., Edmonton, AB, Canada T6G 2E3*

Received 23 February 2001; accepted 19 April 2002

Abstract

Late Pleistocene to Holocene terrestrial climate and vegetation records in the Lower Salmon River Canyon of Idaho are interpreted from the stable isotopic composition of soil carbonates and from aeolian sedimentation frequencies. Carbonate and sediment samples from six sections were processed and analyzed, with the resulting isotopic and grainsize data organized in relation to a normalized time series developed from an associated radiocarbon chronology. This record is interpreted in regards to changes in aridity, temperature and wind speed during the Late Quaternary and is further compared with regional paleoenvironmental records. Lowered $\delta^{18}O$ and $\delta^{13}C$ concentrations before 20 000 yr BP are interpreted as reflecting Late Wisconsinan cold conditions. After 18 000 yr BP, climatic conditions show warmer periods punctuated by sharp returns to colder temperatures and increased C_3 flora by 12 000 yr BP. Higher resolution data show very unstable climatic conditions across the Pleistocene–Holocene boundary, reflected in wide variations in $\delta^{18}O$ and $\delta^{13}C$ and aeolian sand deposition. During the period between 12 000 and 9000 yr BP, the Lower Salmon River Canyon is thought to have experienced marked seasonality with summers and winters, respectively, warmer and colder than today. This climatic scenario was accompanied by an initial instability in canyon vegetation. Following the establishment of a low-energy floodplain in the canyon after 10 000 yr BP, a pattern of C_3-dominant riparian flora appears. During the middle Holocene, climatic and vegetative variability is much reduced from the preceding period. After 4000 yr BP, soil carbonate isotopes reflect a trend toward cooler climate conditions and more mesic vegetation populations.

Keywords: stable isotopes; oxygen-18; carbon-13; loess; paleoclimate; paleovegetation

1. Introduction

Quaternary paleoenvironmental records from the Pacific Northwest are largely derived from studies of pollen records of lakes and bogs in plateau and upland settings (e.g. Mack et al., 1976, 1978a,b, 1979; Mehringer et al., 1977a,b; Hemphill, 1983; Smith, 1983; Barnosky, 1984, 1985; Mehringer, 1985; Foit et al., 1993; Karsian, 1995; Sea and Whitlock, 1995) and montaine glaciers (Kiver 1974; Burke, 1978; Porter, 1978; Da-

* Corresponding author. Present address: 3946 SE Cora St., Portland, OR 97202, USA..

E-mail address: loren_davis@hotmail.com (L.G. Davis).

0031-0182/02/$ – see front matter
PII: S0031-0182(02)00381-4

vis, 1988; Heine, 1998). Despite the large amount of information available from regional paleoenvironmental proxy records, a perspective on Quaternary riparian ecology is largely absent in the Pacific Northwest. Although this is clearly due to the upland location of pollen and glacier studies, one must ask if the conditions reflected in these proxy records are applicable for studies of the nature and timing of vegetative change in riverine contexts. Faced with interpreting the vegetative response of riverine settings to late Quaternary climate change from examples provided in upland paleoenvironmental records, we may be missing important evidence of non-synchronous or unique changes in riparian zones.

In this paper we attempt to construct a high-resolution terrestrial late Pleistocene to Holocene record of climate and vegetation composition in western Idaho through a study of stable oxygen and carbon isotopes in pedogenic carbonate and from grain size variation of loess in the Lower Salmon River Canyon (LSRC). Studies of the stable isotope geochemistry of pedogenic carbonates have been conducted in several areas including central Africa (Cerling, 1992), Nevada (Amundson et al., 1988), Wyoming (Amundson et al., 1996), Texas (Humphrey and Ferring, 1994) and Washington (Stevenson, 1997).

Many investigations of climate from loess grain size variability have been made, particularly in China (e.g. Ding et al., 1991). Our study in the LSRC shows how geologic deposits can be used to develop local-scale paleoclimate and paleovegetation records. Because the floodplain of the Lower Salmon River aggraded for much of the period between 25 000 and 2000 yr BP, a long, high-resolution record of pedogenic carbonate is present where cumulic soils have formed. Loess deposits adjacent to the floodplain offer a contemporaneous record of aeolian grain size variability. Combined, these two records of paleoclimatic and paleovegetation conditions are evaluated from different perspectives. Correlations between datasets are interpreted as revealing a complex record of non-linear interactions among biotic and abiotic components of the LSRC ecosystem, which are compared with other regional paleoenvironmental records.

2. Study area and stratigraphic sections

The LSRC is located approximately 90 km south of Lewiston, Idaho (Fig. 1). Here, extensive Quaternary surficial deposits have been created by alluvial, aeolian, and colluvial processes. Stratigraphic sections used in this study were located in the faces of historic placer mining cuts and in profiles exposed during archaeological excavations conducted in 1997.

In the study area, the Salmon River flows across Triassic metamorphosed basalts, andesites and volcaniclastics of the Wild Sheep Creek Formation (Vallier, 1974), and Tertiary Grande Ronde (Reidel, 1978) and Imnaha basalts (Holden, 1974). During the late Quaternary, structural adjustment along a fault in the downriver portion of the study area roughly parallel to Rock Creek (Gaston and Bennett, 1979), triggered a massive landslide originating from Devils Garden. Basaltic boulder diamict from the slide is widely distributed in the canyon between Rock Creek and American Bar, where it effected a lowering in the gradient of the Salmon River. Late Quaternary deposits predating 10 000 yr BP are dominated by aeolian sedimentation and point bar alluviation (Davis, 2001). After 10 000 yr BP, the Salmon River began a period of nearly continuous floodplain deposition in the study area. At ca. 2000 yr BP the Salmon River incised into the Devils Garden landslide diamict that remained as canyon fill downstream of Rock Creek, resulting in the erosion of its floodplain (Davis, 2001).

Climate summary data are provided in Table 1 for stations in and near the LSRC. Riggins, Idaho, the only station in the canyon and is located about 56 km upriver from the study area, today receives 42.7 cm of annual rainfall with an annual temperature of 19.2°C. Canyon vegetation is primarily composed of grasses (e.g. bluebunch wheatgrass (*Agropyron spicatum*)), annual bromes (*Bromes sp. tectorum*, *Bromes japonicus*, *Bromes brizaeformis*, *Bromes commutatus*, *Bromes rigidus*), and leafy plants like arrowleaf balsamroot (*Balsamorhiza sagittata*) and yarrow (*Achillea millefolium*). Thickets of various shrub species (e.g. hackberry (*Celtus douglasii)*, smooth sumac (*Rhus*

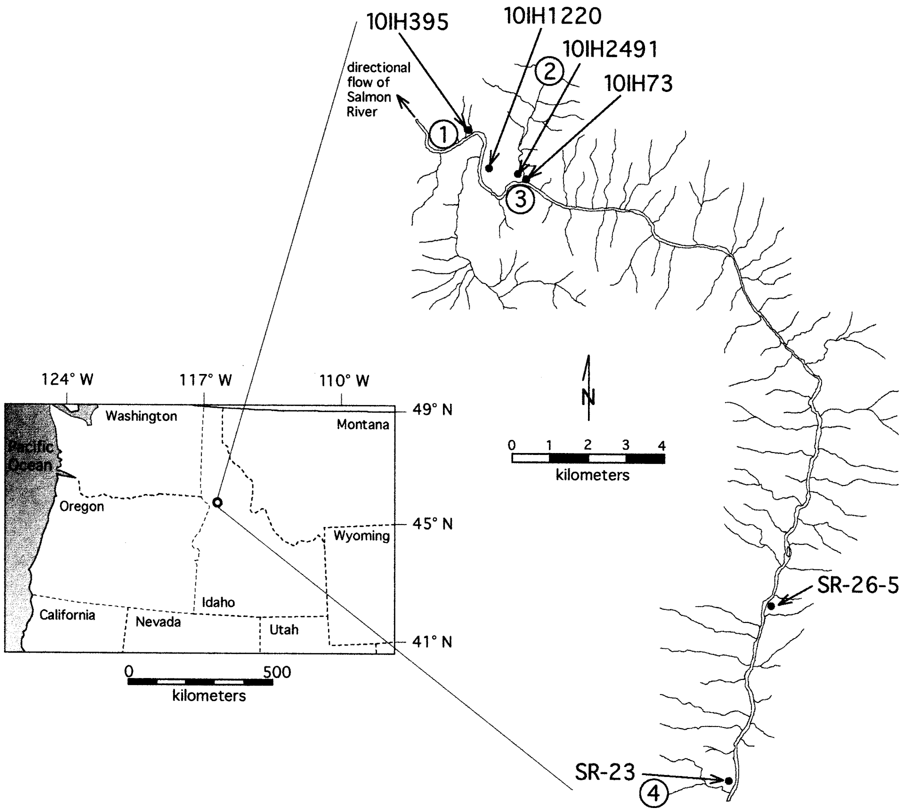

Fig. 1. Location of the LSRC study area in the Pacific Northwest, showing the position of archaeological sites (e.g. 10IH73), stratigraphic sections (e.g. SR-26-5) and other areas mentioned in the text: (1) American Bar; (2) Rock Creek; (3) Devils Garden; (4) Hammer Creek.

glabra), ninebark (*Physocarpus malvaceous*), hawthorn (*Crataegus douglasii*)) and isolated stands of ponderosa pine (*Pinus ponderosa*) and douglas fir (*Pseuduotsuga menziesii*) are seen in tributary drainages with annual or seasonal streamflow and on east and north-facing slopes. The maximum depth of wetting and carbonate precipitation in canyon soils are approximated by the amount of annual rainfall (Jenny, 1941); however, the actual depth of wetting in canyon soils is con-

Table 1
Climatological data from selected stations in and around the Salmon River basin, Idaho (Western Regional Climate Center, 2000)

Station	Annual T	T_{DJF}	T_{MAM}	T_{JJA}	T_{SON}	Annual P	P_{DJF}	P_{MAM}	P_{JJA}	P_{SON}
Cottonwood	13.2	2.6	12.4	24.3	13.6	56.9	12.7	18.3	13.5	12.5
Lewiston	17.4	5.5	16.9	29.7	17.3	32.5	8.4	9.7	7.1	7.6
Boise	17.2	4.4	16.7	30.2	17.7	30.2	10.2	9.4	3.8	7.1
Nezperce	13.8	2.8	12.8	25.3	14.2	53.9	11.9	17.5	11.7	12.7
Grangeville	8.0	−0.7	7.0	17.5	8.2	60.7	11.2	21.6	13.7	14.2
Riggins	19.2	6.9	18.8	31.7	19.3	42.7	9.4	14.2	9.1	10.2

Annual and seasonal (DJF = December, January, February; MAM = March, April, May; JJA = June, July, August; SON = September, October, November) temperature (T) shown in °C. Annual and seasonal precipitation (P) shown in cm.

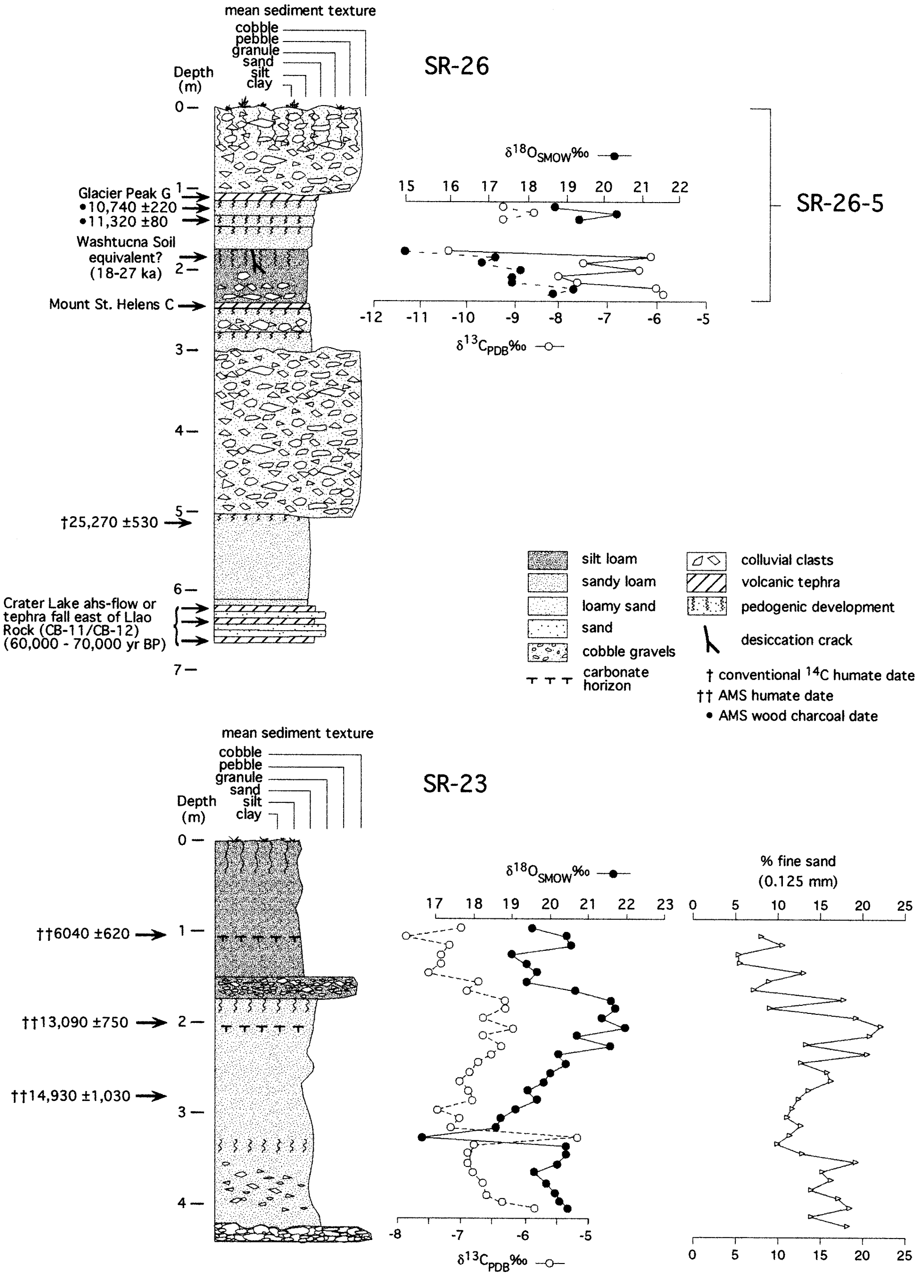

Fig. 2. Profiles of SR-26-5 and SR-23, showing position of stratigraphic units, uncalibrated radiocarbon dates, and stable isotope and grain size values. Closed and open circles represent samples from canyon slope profiles.

siderably less than the amount of precipitation, due to the low intensity and short duration of precipitation events and moderate rates of regional evaporation (i.e. greater than or equal to a range of 148–164 cm mean annual pan evaporation for the study area (United States Environmental Data Service, 1968)). Seasonally, the canyon receives most of its rainfall in the late winter

Table 2
Radiocarbon dates from stratigraphic sections used in this study

Site/section	Provenience	Method	Sample No./C >	Material	Uncalibrated ^{14}C age
10IH2491	2491/D1, D, L4	AMS	Beta-114808	wood char.	1960 ± 40
10IH2491	2491/67, D, L7	AMS	Beta-114805	wood char.	2010 ± 40
10IH2491	2491/50, D, L2	AMS	Beta-114804	wood char.	2050 ± 40
10IH1220	A/7	AMS	TO-7353	char. wood	3070 ± 50
10IH1308	1308/32, 1, L5	Conv.	Tx-9271	mussel shell	3340 ± 60
SR-23	100–110 cm	AMS	TO-7816	soil humate	6040 ± 620
10IH395	120–130 cm	Conv.	Tx-9138	soil humate	6070 ± 60
10IH2491	2491/50, D, L13	AMS	Beta-114806	wood char.	6780 ± 50
10IH1220	250–260 cm	AMS	TO-7815	soil humate	8030 ± 310
10IH395	140 cm	Conv.	Tx-9269	mussel shell	8360 ± 80
10IH73	73/279, A, L7	AMS	Beta-114952	wood char.	8430 ± 70
10IH1220	190–200 cm	AMS	TO-7814	soil humate	9170 ± 180
SR-26	A/1	AMS	TO-7351	char. wood	10 740 ± 220
SR-26	A/2	AMS	TO-7352	char. wood	11 320 ± 90
10IH73	SW/18	AMS	TO-7349	wood char.	11 410 ± 130
SR-23	190–200 cm	AMS	TO-7817	soil humate	13 090 ± 750
SR-23	280–290	AMS	TO-7818	soil humate	14 930 ± 1030
SR-26	505–510 cm	Conv.	Tx-9137	soil humate	25 270 ± 530

and spring months, with hot, dry summers and cool, relatively dry winters.

In order to develop a time-series approach to soil carbonate stable isotopic values and rates of aeolian sedimentation in the study area, stratigraphic sections exhibiting cumulic depositional histories were chosen for study. Two geologic sections and four archaeological sites designated as SR-26-5, SR-23, 10IH73, 10IH395, 10IH1220, and 10IH2491 (Fig. 1) have yielded records of soil carbonate and aeolian sediments spanning the last 25 000 yr BP.

2.1. SR-26-5

An exposure in a large alluvial fan contains multiple deposits of loess, colluvium, alluvial sand and volcanic tephras (Fig. 2). Upper limiting ages for loess deposition are provided by radiocarbon dates of 10 740 ± 220 yr BP (TO-7351) and 11 320 ± 90 yr BP (TO-7352) (Table 2). The presence of a lower oxidized paleosol with desiccation cracks, considered to be a local equivalent to the Late Wisconsinan-age Washtucna Soil identified in the Palouse region of eastern Washington where it is dated between ca. 18 000 and ca. 27 000 yr BP (Busacca and McDonald 1994, Fig. 2), allows for a relative lower limiting age assessment.

2.2. SR-23

Aeolian deposits of carbonaceous silt loam and sandy loam are located on the lower flanks of the canyon near Hammer Creek. These sediments overlie fine to coarse, rounded, mixed-lithology alluvial gravels (Fig. 2) and extend upslope, blanketing colluvium and bedrock in many places. Three AMS dates on soil humate range between 6040 ± 620 yr BP (TO-7816) and 14 930 ± 1030 yr BP (TO-7818) (Table 2). An erosional unconformity is present in the middle of the profile immediately above the position of a 13 090 ± 750 yr BP (TO-7817) humate date.

2.3. 10IH73 Unit A

Archaeological excavations encountered a series of Salmon River floodplain and aeolian deposits separated by sharp boundaries (Fig. 3). Eight radiocarbon dates have been produced from excavation Unit A at 10IH73, although not all are used to establish a chronological framework for site sedimentation (Table 2), due to possible vertical displacement of samples by bioturbation, anthropogenic disturbance and potential contamination of bone samples.

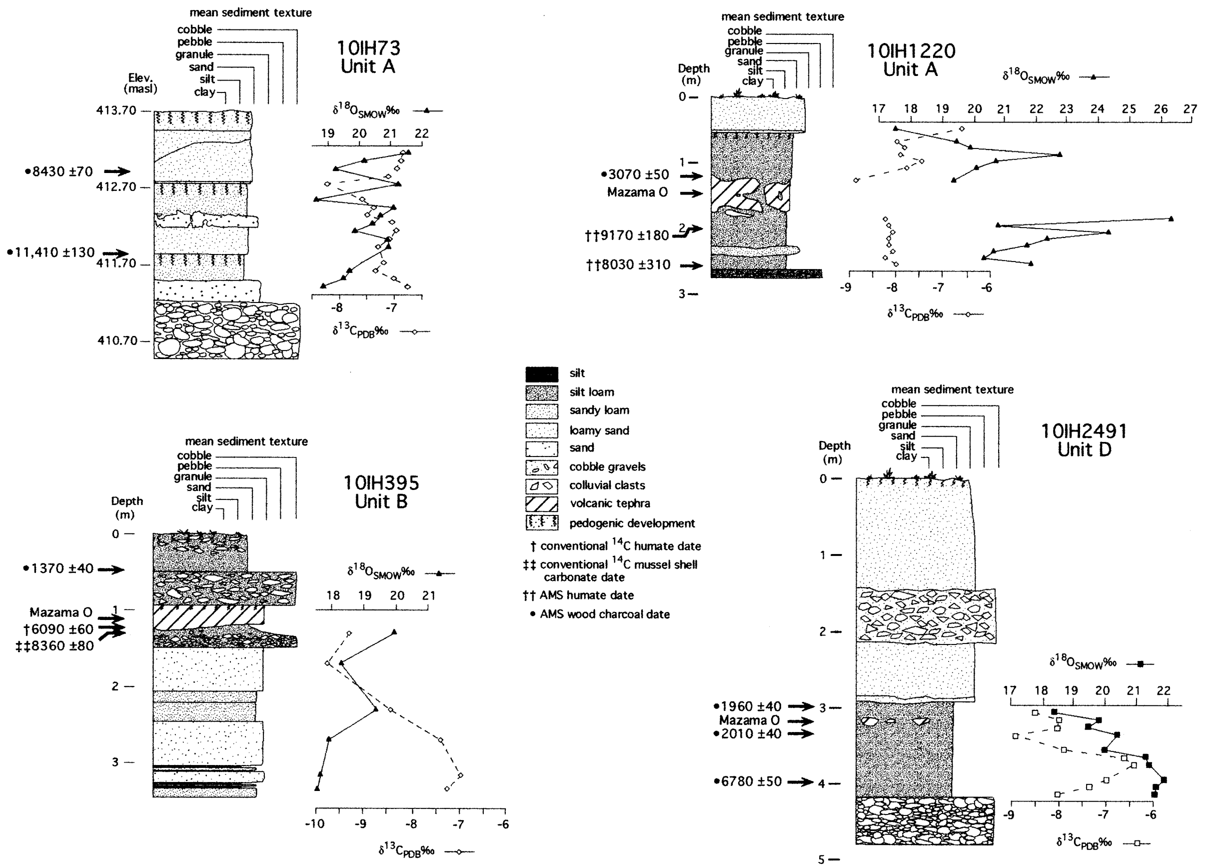

Fig. 3. Profiles of 10IH73 Unit A, 10IH1220 Unit A, 10IH395 Unit B and 10IH2491 Unit D showing position of stratigraphic units, uncalibrated radiocarbon dates, and stable isotope and grain size values. Closed triangles and open diamonds are from Salmon River floodplain sections; closed and open squares are from tributary floodplain deposits.

2.4. 10IH395 Unit B

Stratigraphic profiles in archaeological excavations showed a series of alluvial sands overlain by a silt loam Salmon River floodplain deposit (Fig. 3), which contained a river mussel shell (*Margaritifera falcata*) dated to 8360 ± 80 yr BP (Tx-9269). Erosion of the floodplain occurred after the formation of soil humates at 6090 ± 60 yr BP (Tx-9138), followed by redeposition of Mazama set O tephra and later capped by alluvial fan growth from a nearby tributary drainage.

2.5. 10IH2491 Unit D

This archaeological site produced a Holocene record of tributary floodplain aggradation dating immediately before 6780 ± 50 yr BP (Beta-114806) and lasting until ca. 1960 ± 40 yr BP (Beta-114808) (Table 2). The stratigraphy is comprised of three parts: (1) a basal unit of subangular to subrounded clast-supported boulders; (2) a sandy loam with occasional subrounded to subangular basalt gravel clasts and carbonate filaments; (3) a massive, quartz-rich, medium sand with colluvial clastic content and modern soil development towards the top of the profile (Fig. 3).

2.6. 10IH1220 Unit A

A test pit placed at this archaeological site revealed a stratigraphic sequence of Salmon River floodplain sediments similar to that seen at 10IH2491, dating between 9170 ± 180 yr BP (TO-7814) and 3070 ± 50 yr BP (TO-7353) (Table 2). The four-part stratigraphy encountered here includes: a lower subrounded to subangular gravel unit (1), overlain by silty loam sediments with carbonate filaments (2), that show an erosional contact with a thick unit of redeposited Mazama set O tephra (3), which is buried by more carbonaceous silt loam (4), and a massive medium quartzitic sand (5) (Fig. 3).

3. Methods

3.1. Stable isotopes

Carbonate samples collected at stratigraphic sections from nodules or rhizoliths were examined under low-power microscopy to establish the presence of authigenic carbonate minerals and to look for evidence of diagenesis (e.g. penetration of soil water into nodules through cracks). Soil carbonates were reacted in vacuo with H_3PO_4 at 25.3°C; the resultant CO_2 was cryogenically extracted and analyzed by a Finnegan MAT 252 mass spectrometer, which has an internal error of ±0.1‰ for carbonates. Isotopic concentrations of $\delta^{18}O$ were reported in ‰ relative to standard mean ocean water (Baertschi, 1976) and $\delta^{13}C$ concentrations were reported in ‰ relative to the carbonate standard Peedee Belemnite (Craig, 1957).

3.2. Basis for interpretation

In this study, we assume pedogenic carbonate is formed in equilibrium with soil CO_2 below ca. 20–30 cm in a soil profile (Cerling, 1984), that no significant post-depositional diagenetic change occurred in soil carbonates due to low limits of soil water percolation in the study area, and that the stratigraphic position of soil carbonate in cumulic sedimentation contexts can be related to a time series based on normalized rates of deposition. As well, we follow Cerling (1992), and Cerling and Quade (1993) in their view of the $\delta^{18}O$ signature of soil carbonate as related to the isotopic character of meteoric water, which is influenced by regional precipitation regimes and evaporation of near-surface soil water, and Cerling (1984) by interpreting the $\delta^{13}C$ signature as related to the relative proportion of plants using the C_4 photosynthetic pathway.

Cerling (1992), and Cerling and Quade (1993) explain correlations between $\delta^{18}O$ and $\delta^{13}C$ concentrations in soil carbonate as a result of temperatures and aridity affecting plants with the C_3 photosynthetic pathway. Decreased $\delta^{18}O$ and $\delta^{13}C$ reflect more temperate conditions. This occurs as lowered atmospheric temperatures deplete $\delta^{18}O$ in meteoric water during more frequent precipitation events, and fractionation effects on pedogenic carbonate fractionation occur under lower soil temperatures. Under more xeric conditions, the opposite effect is expected. Under this scenario, greater $\delta^{18}O$ concentration in rainfall resulting from fewer precipitation events, is combined with increased soil temperatures and rates of evaporation in near-surface soil water to produce heightened $\delta^{18}O$ concentration in soil carbonates (Cerling, 1992; Cerling and Quade, 1993). Just as increased concentrations of $\delta^{18}O$ in soil carbonate are associated with arid conditions, rising $\delta^{13}C$ values reflect the expansion of drought-tolerant C_4 plants at the expense of their more mesic C_3 counterparts (Cerling, 1992). Relating the isotopic signature of soil carbonates to climatic conditions assumes a consistent source of precipitation. In cases where shifting atmospheric circulation patterns bring meteoric water from different sources through time, resultant soil carbonate $\delta^{18}O$ records are not thought to represent proxy paleoclimatic indicators (e.g. Amundson et al., 1996). In our study area, meteoric water is derived almost exclusively from Pacific westerlies, and has likely been the case throughout the late Quaternary. Thus, it is difficult to reconcile soil carbonate $\delta^{18}O$ records from regions with different precipitation sources.

Study of shallow groundwater $\delta^{18}O$ and δD in the area of Pullman, Washington and Moscow, Idaho, USA by Larson (1996) established a local meteoric water line, with a slope of $\delta D = \delta^{18}O\,(6.68) - 18.62$. Using O'Neil et al's (1969) equation describing the relationship between the $\delta^{18}O$ of water and calcite, the isotopic values of LSRC

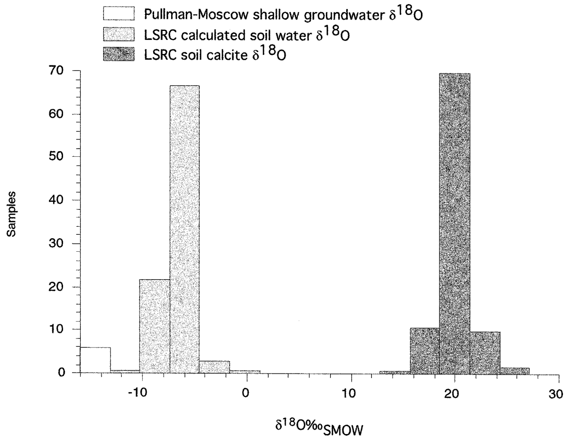

Fig. 4. Comparison of the stable oxygen isotope composition of Pullman–Moscow shallow groundwater (Larson, 1996), LSRC soil water, and LSRC soil calcite. Assuming a mean summer temperature of 31.7°C (same as Riggins, Idaho), the $\delta^{18}O$ of the soil water that LSRC calcite formed from is calculated as 26.6‰, following the method of O'Neil et al. (1969). Variance in LSRC soil water is established by difference between the calculated soil water value and the $\delta^{18}O$ of LSRC soil calcite. This graph shows a progressive enrichment of $\delta^{18}O$ in Pullman–Moscow shallow groundwater, LSRC soil water, and LSRC soil calcite, highlighting the role of local evaporation in the fractionation of LSRC soil carbonates.

soil water and soil carbonates were calculated and plotted relative to Pullman–Moscow Basin meteoric water $\delta^{18}O$ values (Fig. 4). The relative isotopic enrichment of LSRC soil water and soil carbonates relative to Pullman–Moscow Basin shallow groundwater points to the influence of evaporation in the fractionation process (Welhan, 1987, Fig. 1). Because local geographic conditions in the study area influence rates of solar insolation, soil water availability, and evaporation we expect that soil carbonates of the same age collected from different parts of the canyon (e.g. north-facing versus south-facing slopes, or well-drained loess deposits on slopes versus well-watered alluvial floodplains) will show synchronic variability in $\delta^{18}O$ composition, which reflect the differential operation of microclimatic and hydrological processes. Thus, the overall trend of soil carbonate $\delta^{18}O$ variability gives a detailed perspective on canyon paleoenvironments.

3.3. Aeolian grain size variability

Extensive deposits of sandy loess from SR-23 were sampled for granulometric analysis. Sediment samples were first oven-dried at 60°C for 24 h. The dried samples were carefully disaggregated by hand in a mortar and 100 g of sediment was passed through a series of US Standard wire mesh sieves to separate coarse sand to silt-sized fractions (+1 to +4 phi; US Standard Sieve sizes 35, 60, 120, 230 and pan) (after Wentworth, 1922). Each stack of sieves was mechanically shaken for 15 min with resulting size fractions weighed individually.

3.4. Basis for interpretation

Canyon sediments were identified as aeolian in origin based on multiple criteria, including their lack of stratification or bedding structures, angle of repose (typically greater than 10%), dominance of fine sand- to silt-sized particles, clastic surface morphology, and calcium carbonate content. Sediments deposited in the floodplain zone of the Lower Salmon River would have provided a material source for short-distance aeolian transport, resulting in the accumulation of sandy loess on the lower flanks of the canyon (cf. Pye, 1995). This model of aeolian transport is supported by scanning electron microscopy, which shows abrasion and fracturing on the edges and faces of angular to subangular sand grains (Fig. 5). On this basis, the frequency of grain size classes in SR-23 aeolian sediments are organized in a time series and evaluated to reveal potential paleoclimatic indicators; this mode of reasoning has been used to interpret aeolian sedimentation records in China's Loess Plateau (e.g. Ding et al., 1991).

3.5. Establishing a time series

Radiocarbon dates produced from the six study sections form the primary basis for placing isotope and grain size samples in a temporal context (Table 2). In order to organize the isotope and grain size samples in a time series, sedimentation rates have been interpolated from the stratigraphic depth of radiocarbon dates. In the case of the

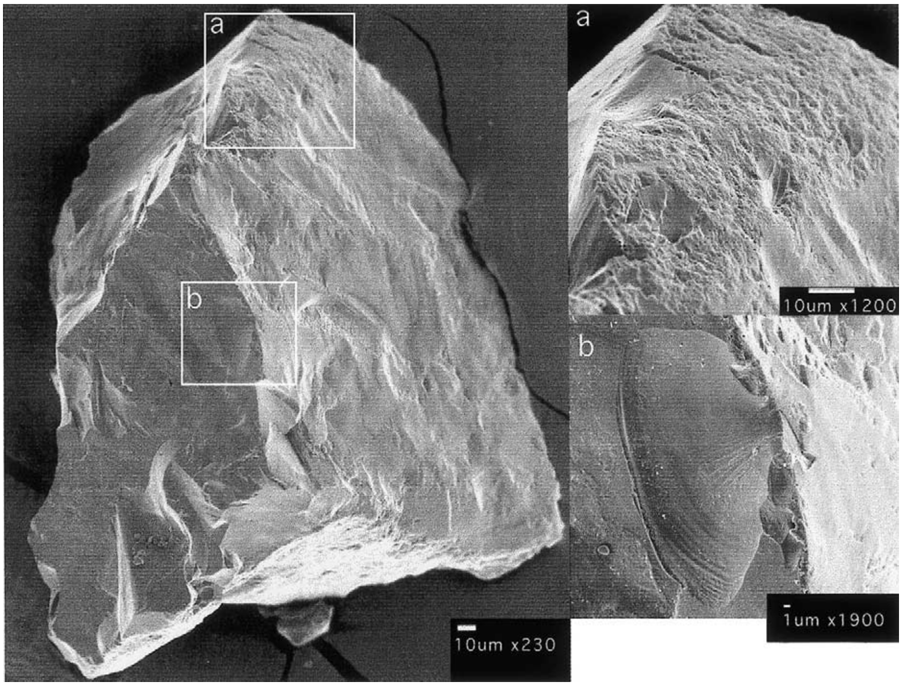

Fig. 5. Representative SEM images of sand grain morphology from SR-23. Detail of abrasion (a) and conchoidal fracturing (b).

SR-26-5 section, the presence of a paleosol likely formed under late Wisconsinan environmental conditions (Davis, 2001) provided a relative age marker. Considering the limited depth of soil wetting in the study area we used a 20 cm depth of precipitation for soil carbonates. By shifting the stratigraphic position of soil carbonate samples upwards by 20 cm we adjusted for temporal asynchroneity. In the case of grain size samples from SR-23 no adjustment was made as the vertical position of samples can be directly related to a normalized time series. A few minor adjustments were made to the chronological framework after comparing temporally corresponding isotopic and grain size records of different sections in order to attain a better fit among datasets and to aid in the graphical presentation of the data.

4. Results and discussion

Soil carbonate isotopes from all sections (Tables 3 and 4) have a total range in $\delta^{18}O$ of 11.3‰ (from 15.0 to 26.3‰). The greatest variation in $\delta^{18}O$, in any one section, was seen at 10IH1220, which spanned 8.8‰ (from 17.5 to 26.3‰). Total variation in $\delta^{13}C$ covered 5.2‰ (from −10.4 to −5.2‰) with the largest variability of all sections seen at SR-26-5 covering 4.5‰ (from −10.4 to −5.9‰).

Sections positioned on canyon slopes (SR-26-5 and SR-23) and in tributary floodplains (10IH2491) show stronger positive covariation between $\delta^{18}O$ and $\delta^{13}C$ (Fig. 6) than among Salmon River floodplain sections, with greater proportions of C_4 plants appearing on slopes during periods of increased $\delta^{18}O$ concentration. This positive covariation is interpreted as the direct effect of xeric climate conditions on canyon vegetation. Soil carbonates from 10IH73 and 10IH2491 have a low correlation between $\delta^{18}O$ and $\delta^{13}C$, suggesting that the proportion of C_4 plants in the Salmon River floodplain zone is not directly influenced by climatic effects. Our interpretation of this riparian pattern is that water retained in the finer floodplain sediments and the underlying groundwater zone provides an adaptive buffer for phreatophytic and mesic plants, allowing for the mainte-

Table 3
Stable isotope geochemistry results from SR-26-5, 10IH73, 10IH2491, 10IH1220 and 10IH395

Stratigraphic section	Depth (cm) BD	Elevation (masl)	Soil $\delta^{18}O$ (‰)	Soil $\delta^{13}C$ (‰)
SR-26	10		18.7	−9.3
SR-26	20		20.3	−8.5
SR-26	30		19.4	−9.3
SR-26	80		15.0	−10.4
SR-26	90		17.2	−6.1
SR-26	100		16.8	−7.5
SR-26	110		17.9	−6.3
SR-26	120		17.6	−8.0
SR-26	130		17.6	−7.6
SR-26	140		19.3	−6.0
SR-26	150		18.5	−5.9
10IH73		413.10	21.6	−6.9
10IH73		413.00	20.1	−6.9
10IH73		412.90	19.2	−7.0
10IH73		412.80	20.2	−7.1
10IH73		412.70	21.2	−8.2
10IH73		412.50	18.6	−7.6
10IH73		412.40	21.1	−7.4
10IH73		412.30	20.7	−7.5
10IH73		412.20	20.4	−7.1
10IH73		412.10	19.8	−7.0
10IH73		412.00	20.9	−7.1
10IH73		411.90	20.9	−7.3
10IH73		411.70	20.0	−7.2
10IH73		411.60	19.7	−7.4
10IH73		411.50	19.5	−7.0
10IH73		411.40	18.8	−6.8
10IH2491	50		18.2	−8.6
10IH2491	60		19.4	−8.1
10IH2491	70		19.1	−8.2
10IH2491	80		20.0	−8.9
10IH2491	100		19.6	−8.0
10IH2491	110		20.7	−7.0
10IH2491	120		20.8	−6.8
10IH2491	140		21.2	−7.3
10IH2491	150		21.0	−7.6
10IH2491	160		21.0	−8.2
10IH1220	50		17.5	−6.6
10IH1220	60		19.4	−7.9
10IH1220	70		19.0	−7.7
10IH1220	80		19.9	−7.8
10IH1220	90		22.7	−7.9
10IH1220	100		20.7	−7.5
10IH1220	110		20.1	−7.8
10IH1220	130		19.4	−8.9
10IH1220	190		26.3	−8.3
10IH1220	200		20.8	−8.2
10IH1220	210		24.3	−8.1
10IH1220	220		22.4	−8.2
10IH1220	230		21.7	−8.2
10IH1220	240		20.6	−8.1
10IH1220	250		20.3	−8.3

Table 3 (*Continued*).

Stratigraphic section	Depth (cm) BD	Elevation (masl)	Soil $\delta^{18}O$ (‰)	Soil $\delta^{13}C$ (‰)
10IH1220	260		21.8	−7.9
10IH395	130		20.0	−9.3
10IH395	170		18.3	−9.8
10IH395	230		19.4	−8.5
10IH395	270		17.9	−7.4
10IH395	316		17.7	−7.0
10IH395	335		17.6	−7.3

Depth is reported in centimeters below datum (BD) and as elevation in masl. Depth or elevation intervals with no isotopic data are omitted.

nance of higher C_3 populations during xeric periods. While vegetation patterns in areas lacking a constant or reliable water source are seen to shift rapidly and in proportion to climate changes, the flora of the Salmon River riparian zone appears to have changed very little through time.

Isotopic values organized in a time series show the relationship between climate and vegetation patterns in the LSRC (Fig. 7). In the case of 10IH73, the trend in $\delta^{13}C$ concentration lags behind the pattern of $\delta^{18}O$ values. This is thought to be linked to an asynchronous relationship between climate conditions and hydrological response in the floodplain. The isotopic data from 10IH1220 suggests that where the gradient of the Salmon River channel has been greatly reduced, soil water may have been more plentiful for plant growth in the floodplain during most of the Holocene, thus no lead-lag pattern is seen. Data from 10IH2491 shows that tributary floodplains were more prone to desiccation, as evidenced by a closer covariance between $\delta^{18}O$ and $\delta^{13}C$. This is expected as few tributary canyons in the study area maintain perennial streamflow today, and of those, discharge is extremely reduced during the summer months.

4.1. Late Pleistocene environments

An initial period of cold and wet conditions is seen before ca. 20 000 yr BP, associated with a flora almost entirely composed of C_3 plants. Between ca. 17 000 and ca. 15 700 yr BP, fine sand deposition fluctuates between 15 and 20% at SR-23, suggesting a period of heightened aridity. De-

Table 4
Stable isotopic concentration of soil carbonate, fine sand frequency at SR-23

Depth cm (BS)	Soil $\delta^{18}O$ (‰)	Soil $\delta^{13}C$ (‰)	% Fine sand
110	19.5	−7.0	10.4
120	20.4	−7.9	5.3
130	20.6	−7.2	5.4
140	19.0	−7.3	13.0
150	19.4	−7.3	8.9
160	19.6	−7.5	7.1
170	19.4	−6.7	17.6
180	20.7	−6.9	9.0
190	21.6	−6.3	19.1
200	21.7	−6.3	22.1
210	21.4	−6.6	20.8
220	21.9	−6.2	13.3
230	20.7	−6.6	20.4
240	21.6	−6.4	12.6
250	20.2	−6.5	15.8
260	20.4	−6.7	16.2
270	20.0	−6.9	13.5
280	19.8	−7.0	12.3
290	19.4	−6.9	11.6
300	19.7	−6.8	11.1
310	19.1	−7.4	12.6
320	18.7	−7.0	11.4
330	18.6	−7.2	9.8
340	16.7	−5.2	12.8
350	20.4	−6.8	19.1
360	20.4	−6.9	15.1
370	20.2	−6.9	16.2
380	19.6	−6.8	13.9
390	19.9	−6.7	17.0
400	20.1	−6.6	18.4
410	20.2	−6.4	13.9
420	20.5	−5.8	18.1

Depth is reported in centimeters below surface of profile.

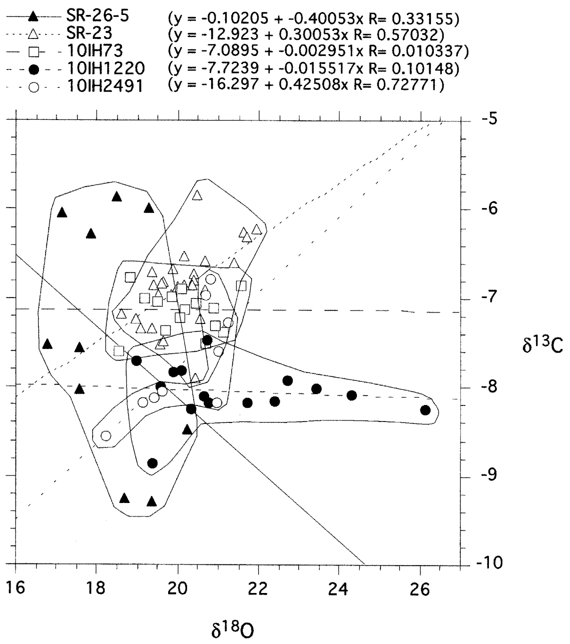

Fig. 6. Cross plot of soil carbonate $\delta^{18}O$ versus $\delta^{13}C$ for all stratigraphic profiles.

clining $\delta^{18}O$ concentrations point to a return to colder and wetter climates between ca. 16 000 and ca. 14 500 yr BP, which is matched by a reduced fine sand influx. Fine sand deposition and $\delta^{18}O$ values rise between ca. 14 500 and 12 300 yr BP, marking a drying trend. Canyon slopes show a reduction of C_3 flora after ca. 17 000 yr BP, continuing on until 14 000 yr BP. Immediately after 12 000 yr BP, $\delta^{18}O$ plunges, followed by a sharp decline in $\delta^{13}C$ concentration, suggesting a brief and rapid resurgence of cold conditions. These changes in canyon proxy records closely approximate the timing and magnitude of the European Younger Dryas climate event, as seen in Europe, North America, and elsewhere (e.g. Berglund, 1979; Overpeck et al., 1989; Engstrom et al., 1990; Flower and Kennett, 1990; Linsley and Thunell, 1990; Kudrass et al., 1991; Mathewes et al., 1993; Peteet et al., 1990; Reasoner et al., 1994).

4.2. *Late Pleistocene–early Holocene transition environments*

Between 11 000 and 10 000 yr BP, $\delta^{18}O$ and $\delta^{13}C$ values show unstable climatic and vegetation patterns, swinging widely from warmer and drier conditions at ca. 10 500 yr BP to colder and wetter conditions at ca. 10 000 yr BP. Greater vegetative stability is seen between 10 000 and 9000 yr BP as $\delta^{13}C$ concentrations show little variability compared to the broad fluctuations in corresponding $\delta^{18}O$. Immediately before 11 310 ± 80 yr BP (TO-7358) the Lower Salmon River began to build a broad floodplain, evidence of which is widespread in the study area by ca. 10 000 yr BP (Davis, 2001), and is thought to have contributed to increased C_3 percentages at 10IH1220 and 10IH73. We agree with Elias (1996) who, on the basis of fossil beetle assemblages in the Rocky Mountains region, finds evidence of a thermal maximum during the terminal Pleistocene–early Holocene period.

4.3. *Middle Holocene environments*

Variability in $\delta^{13}C$ is lower on canyon slopes and in tributary floodplains between 9000 and 5700 yr BP than during the previous period. Although Salmon River floodplain isotopic data are largely absent here, the generally lower $\delta^{13}C$ concentrations noted in tributary floodplains between ca. 8500 and 6000 yr BP suggests similar trends may be occurring on the Salmon River floodplain. On average, terminal Pleistocene–early Holocene $\delta^{18}O$ and $\delta^{13}C$ is higher and lower than seen during the middle Holocene period. This is interpreted as the result of increased solar insolation in July and decreased insolation in January between 11 000 and 9000 yr BP than between 9000 and 5000 yr BP (Berger, 1978).

4.4. *Late Holocene environments*

After 5000 yr BP, $\delta^{13}C$ values fall in tributary floodplain deposits, showing a reduction in the percentage of C_4 flora. This pattern is paralleled by declining $\delta^{18}O$ concentrations, suggesting the growing presence of cooler and wetter climatic conditions. By the end of the record at 2000 yr BP, $\delta^{18}O$ values are at their lowest since the terminal Pleistocene. A sharp rise in $\delta^{13}C$ at 10IH1220 is related to the incision of the Salmon

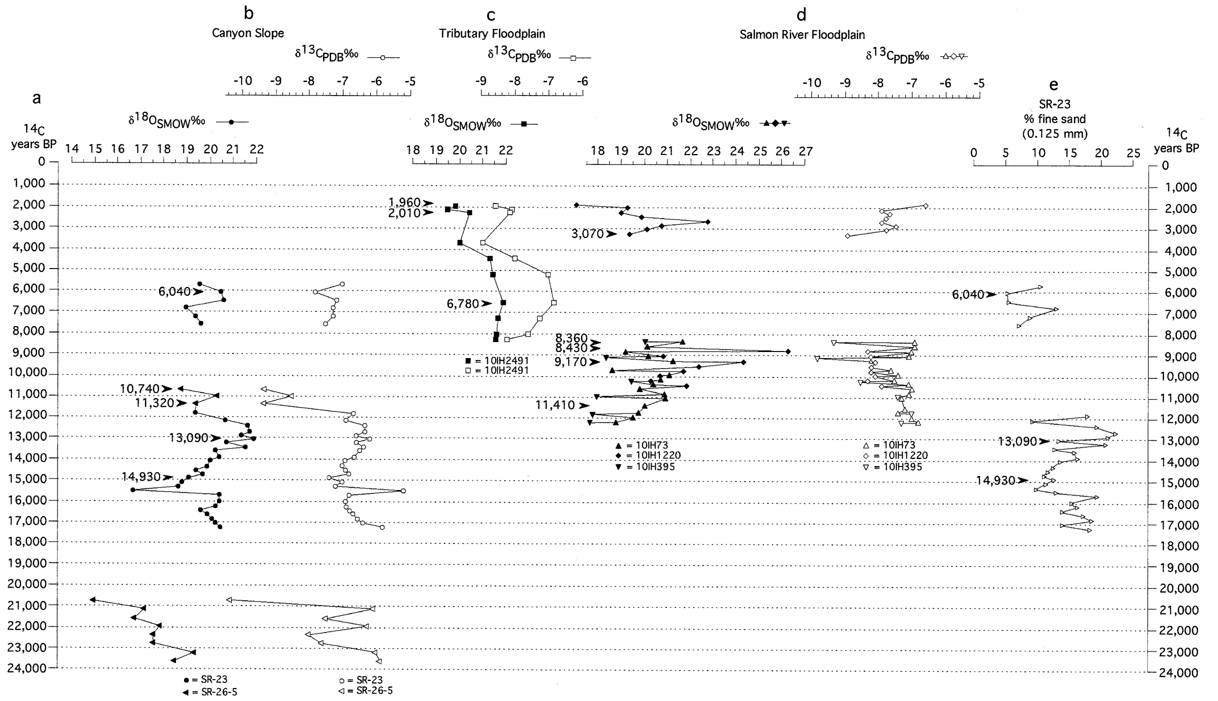

Fig. 7. Chronology (a) (in uncalibrated ^{14}C years BP) of LSRC soil carbonate δ^{18}O and δ^{13}C from canyon slope (b), tributary floodplain (c), and Salmon River floodplain (d) contexts, compared to aeolian fine sand percentages from SR-23 (e). Solid lines follow variation in δ^{18}O, δ^{13}C, and fine sand. Symbol keys are provided beneath plotted data. Arrows show positions of radiocarbon dates to left of plots.

River channel into its floodplain (Davis, 2001), which lowered the water table, favoring drought-resistant C_4 plants. Today, the LSRC floodplain is much smaller than its pre-2000 BP condition while modern riparian vegetation cover is likewise reduced. Although modern climate conditions are relatively cooler and more mesic compared to paleoenvironmental records, canyon riparian ecosystems of the interior Columbia River basin retain far less vegetative biomass than under warmer and drier regimes prior to 2000 BP. This situation is likely due to late Holocene alluvial baselevel changes that reduced the size of floodplains and altered soil water regimes that previously supported higher populations of phreatophytic vegetation.

4.5. Comparison with regional paleoenvironmental records

In a series of papers, Mack et al. (1976, 1978a,b, 1979) provide a view of postglacial vegetation change in northeast Washington and northern Idaho. Although some pollen cores were taken from areas within river valleys, little detail on the nature of riparian and slope vegetation can be provided. Instead, general statements about changing vegetation populations as indicators of paleoclimatic conditions are given. These studies illustrate difficulties pollen studies have in differentiating specific geographic sources of pollen, particularly as they relate to the distribution of plants in a landscape (e.g. riparian versus slope).

Mehringer's (1996) discussion of paleovegetation records from middle Rocky Mountain ecoregion sources (Mehringer et al., 1977a,b, 1984; Hemphill, 1983; Foit et al., 1993; Karsian, 1995) provides a summary of palynological studies near the LSRC. Of these regional records, only Blue Lake (Smith, 1983) lies close to the elevation of the bottom of the LSRC (1035 m above sea level (masl) versus ca. 1000 masl, respectively); however, the pollen record from Blue Lake only spans the last 4300 BP. The remaining bogs and ponds are located at much higher elevations, between 1630 and 2152 masl. Mehringer (1996) summarizes the record of vegetation change in the middle Rocky Mountain ecoregion in the following manner: (1) before the eruption of Glacier Peak tephra at 11 200 BP, subalpine conifers populate high elevations near Lost Trail Pass Bog, denoting existing cold conditions; (2) before the airfall of Mazama tephra (6850 BP), grass and sagebrush, and Douglas-fir and lodgepole pine replace cold-tolerant whitebark pine, marking an upslope movement of xerothermic plants in response to postglacial warming; (3) continued expansion of Douglas-fir upslope into higher elevations is equated with middle Holocene warming; (4) by 5000 BP, whitebark and lodgepole pines increase at expense of Douglas-fir, signalling the onset of cooler conditions; (5) after 1750 BP, vegetation populations are similar to today's cooler conditions.

The view from pollen records in the southern Plateau, central Idaho, and middle Rocky Mountains gives little insight on the history of riparian vegetation. Because they are largely derived from plant populations situated in well-drained upland contexts, pollen records from the region surrounding the LSRC are best compared with $\delta^{13}C$ proxy records of vegetation from canyon slopes, which show a close responsive relationship with changing climatic conditions. Regional pollen records do not reveal an asynchronous relationship between riparian vegetation and climate conditions, however, revealing only half of the picture seen in LSRC records. The stability of LSRC riparian vegetation under rising postglacial temperatures and aridity is unique among regional paleoenvironmental records reviewed here and likely reflects the complexity and productivity of regional riparian vegetation during the postglacial period.

Corroborating evidence of increased postglacial riparian productivity in the Plateau region comes from Hammatt's (1976) study of late Quaternary stratigraphy and geomorphology in the Lower Granite Reservoir stretch of southeastern Washington's Lower Snake River Canyon. On the basis of lithostratigraphic and pedostratigraphic evidence, Hammatt (1976) interprets the development of a floodplain with lush, C_3-dominated riparian vegetation by 8000 BP. As with the LSRC record, growing productivity among riparian plant populations in the canyonlands of the interior Pacific Northwest during the late Pleistocene to middle Holocene period is not expected given the basis of postglacial climate and upland paleovegetation change.

5. Conclusions

Stable isotopic concentrations in soil carbonates and grainsize frequencies in aeolian sediments are interpreted here to reflect regional and local changes in late Pleistocene to Holocene climate conditions, and vegetative populations of riparian and slope areas of the LSRC. The approaches used in this study offer a means of inferring paleoenvironmental conditions from lesser-known lowland Plateau contexts. This study has also discovered the operation of highly variable climate conditions across the late Pleistocene to early Holocene (cf. Taylor et al., 1993), and an asynchronous vegetation–climate relationship in canyon riparian zones, which reflect an important degree of late Quaternary ecosystemic complexity. The construction of high-resolution records of paleovegetation and paleoclimate from locally available proxy sources has direct applications in archaeological, geoarchaeological and paleoenvironmental studies of semi-arid and arid locales in the Far West. At this time, studies of this kind are notably uncommon at detailed late Pleistocene to Holocene temporal scales.

Acknowledgements

Funding for this research was provided through a challenge cost share agreement between the Bureau of Land Management and the University of Alberta. Special thanks to David Sisson for his administrative support and help in arranging fieldwork sessions. We also wish to thank Patrick

De Deckker, Oliver Chadwick, and Owen Davis for their helpful comments on an earlier version of this paper. This paper presents some of the results of Ph.D. dissertation research supported by a Ph.D. Scholarship and a Dissertation Fellowship of the University of Alberta granted to L.G.D.

References

Amundson, R., Chadwick, O., Kendall, C., Wang, Y., DeNiro, M., 1996. Isotopic evidence for shifts in atmospheric circulation patterns during the late Quaternary in mid-North America. Geology 24, 23–26.

Amundson, R.G., Chadwick, O.A., Sowers, J.M., Doner, H.E., 1988. Relationship between climate and vegetation and the stable carbon isotope geochemistry of soils in the eastern Mojave desert, Nevada. Quat. Res. 29, 245–254.

Baertschi, P., 1976. Absolute ^{18}O content of standard mean ocean water. Earth Planet. Sci. Lett. 31, 341.

Barnosky, C.W., 1984. Late Pleistocene and early Holocene environmental history of southwestern Washington State, USA. Can. J. Earth Sci. 21, 619–629.

Barnosky, C.W., 1985. Late Quaternary vegetation in the southwestern Columbia Basin, Washington. Quat. Res. 23, 109–122.

Berger, A.L., 1978. Long-term variations in caloric insolation resulting from the Earth's orbital elements. Quat. Res. 9, 139–167.

Berglund, B.E., 1979. The deglaciation of southern Sweden 13 500–10 000 BP. Boreas 8, 89–117.

Burke, R.M., 1978. Comparison of relative age dating (RAD) data from eastern Sierra Nevada cirque deposits with those from the tephrochronologically age controlled deposits of the Wallowa Mountains, Oregon. Geol. Soc. Am. Abstr. Programs 10, 211.

Busacca, A.J., McDonald, E.V., 1994. Regional sedimentation of late Quaternary loess on the Columbia Plateau: sediment source areas and loess distribution patterns. Wash. Div. Geol. Earth Resour. Bull. 80, 181–190.

Cerling, T.E., 1984. The stable isotopic composition of modern soil carbonate and its relationship to climate. Earth Planet. Sci. Lett. 71, 229–240.

Cerling, T.E., 1992. Development of grasslands and savannas in eastern Africa during the Neogene. Palaeogeogr. Palaeoclimatol. Palaeoecol. 97, 241–247.

Cerling, T.E., Quade, J., 1993. Stable carbon and oxygen isotopes in soil carbonates. Climate change in continental records. Geophys. Monogr. 78, 217–231.

Craig, H., 1957. Isotopic standards for carbon and oxygen and correction factors for mass-spectrometric analysis of carbon dioxide. Geochim. Cosmochim. Acta 12, 133–149.

Davis, L.G., 2001. The Coevolution of Early Hunter–Gatherer Culture and Riparian Ecosystems in the Southern Columbia River Plateau. Unpublished Ph.D. dissertation, Department of Anthropology and Department of Earth and Atmospheric Sciences, University of Alberta, Edmonton, AB.

Davis, P.T., 1988. Holocene glacier fluctuations in the American Cordillera. Quat. Sci. Rev. 7, 129–157.

Ding, Z.L., Rutter, N., Liu, T.S., Evans, M.E., Wang, Y.C., 1991. Climatic correlation between Chinese loess and deep-sea cores: a structural approach. In: Liu, T. (Ed.), Loess, Environment and Global Change. Science Press, Beijing, pp. 168–186.

Elias, S.A., 1996. Late Pleistocene and Holocene seasonal temperatures reconstructed from fossil beetle assemblages in the Rocky Mountains. Quat. Res. 46, 311–318.

Engstrom, D.R., Hanses, B.C.S., Wright, H.E., Jr., 1990. A possible Younger Dryas record in southeastern Alaska. Science 250, 1383–1385.

Flower, B.P., Kennett, J.P., 1990. The Younger Dryas cool episode in the Gulf of Mexico. Paleoceanography 5, 949–961.

Foit, F.F., Jr., Mehringer, P.J., Jr., Sheppard, J.C., 1993. Age, distribution and stratigraphy of Glacier Peak tephra in eastern Washington and western Montana, USA. Can. J. Earth Sci. 30, 535–552.

Gaston, M.P., Bennett, E.H., 1979. Geologic Map of the Grangeville Quadrangle, Idaho. Idaho Bureau of Mines and Geology, Moscow, ID.

Hammatt, H.H., 1976. Late Quaternary Stratigraphy and Archaeological Chronology in the Lower Granite Reservoir, Lower Snake River, Washington. Ph.D. dissertation, Washington State University, Pullman, WA.

Heine, J.T., 1998. Extent, timing, and climatic implications of glacier advances on Mount Rainier, Washington, USA, at the Pleistocene/Holocene transition. Quat. Sci. Rev. 17, 1139–1148.

Hemphill, M.L., 1983. Fire, Vegetation, and People: Charcoal and Pollen Analyses of Sheep Mountain Bog, Montana: the Last 2800 Years. M.A. thesis, Washington State University, Pullman, WA.

Holden, G.S., 1974. Chemical and Petrographic Stratigraphy of the Columbia River Basalt in the Lower Salmon River Canyon, Idaho. M.Sc. thesis, Washington State University, Pullman, WA.

Humphrey, J.D., Ferring, C.R., 1994. Stable isotopic evidence for latest Pleistocene and Holocene climatic change in north-central Texas. Quat. Res. 41, 200–213.

Jenny, H., 1941. Factors of Soil Formation: a System of Quantitative Pedology. McGraw-Hill, New York.

Karsian, A.E., 1995. A 6800-year vegetation and fire history in the Bitterroot Mountain Range, Montana. M.Sc. thesis, University of Montana, Missoula, MT.

Kiver, E.P., 1974. Holocene glaciation in the Wallowa Mountains, Oregon. In: Mahaney, W.C. (Ed.), Quaternary Environments: Proc. Symp. Geographical Monographs 5. York University-Atkinson College, Toronto, ON, pp. 169–195.

Kudrass, H.R., Erienkeuser, H., Vollbrecht, R., Weiss, W., 1991. Global nature of the Younger Dryas cooling event inferred from oxygen isotope data from Sulu Sea cores. Nature 349, 406–408.

Larson, K.R., 1996. Stable Isotopes in the Pullman–Moscow Basin, Eastern Washington and North Idaho: Implications for the Timing, Magnitude and Distribution of Groundwater Recharge. M.Sc. thesis, Washington State University, Pullman, WA.

Linsley, B.K., Thunell, R.C., 1990. The record of deglaciation in the Sulu Sea: evidence for the Younger Dryas event in the tropical west Pacific. Paleoceanography 5, 1025–1039.

Mack, R.N., Bryant, V.M., Jr., Fryxell, R., 1976. Pollen sequences from the Columbia Basin, Washington: reappraisal of postglacial vegetation. Am. Midl. Nat. 95, 390–397.

Mack, R.N., Rutter, N.W., Bryant, V.M., Jr., Valastro, S., 1978a. Reexamination of postglacial vegetation history in northern Idaho: Hager Pond, Bonner County. Quat. Res. 10, 241–255.

Mack, R.N., Rutter, N.W., Valastro, S., Bryant, V.M., Jr., 1978b. Late Quaternary vegetation history at Waits Lake, Colville River Valley, Washington. Bot. Gaz. 139, 499–506.

Mack, R.N., Rutter, N.W., Valastro, S., 1979. Holocene vegetation history of the Okanogan Valley, Washington. Quat. Res. 12, 212–225.

Mathewes, R.W., Heusser, L.E., Patterson, R.T., 1993. Evidence for a Younger Dryas-like cooling event on the British Columbia coast. Geology 21, 101–104.

Mehringer, P.J., Jr., 1985. Late-Quaternary pollen records from the interior Pacific Northwest and northern Great Basin of the United States. In: Bryant, V.A., Holloway, R.G. (Eds.), Pollen Records of Late-Quaternary North American Sediments. American Association of Stratigraphic Palynologists, Dallas, TX, pp. 167–189.

Mehringer, P.J., Jr., 1996. Columbia River basin ecosystems: Late Quaternary environments. Report prepared for the Interior Columbia Basin Ecosystem Management Project. Available at http://www.icbemp.gov/science/scirpte.html.

Mehringer, P.J., Jr., Arno, S.F., Petersen, K.L., 1977a. Postglacial history of Lost Trail Pass Bog, Bitterroot Mountains, Montana. Arct. Alp. Res. 9, 345–368.

Mehringer, P.J., Jr., Blinman, E., Petersen, K.L., 1977b. Pollen influx and volcanic ash. Science 198, 257–261.

Mehringer, P.J., Jr., Sheppard, J.C., Foit, F.F., Jr., 1984. The age of Glacier Peak tephra in west-central Montana. Quat. Res. 21, 36–41.

O'Neil, J.R., Clayton, R.N., Mayeda, T.K., 1969. Oxygen isotope fractionation in divalent metal carbonates. J. Chem. Phys. 51, 5547–5558.

Overpeck, J.T., Peterson, L.C., Kipp, N., Imbrie, J., Rind, D., 1989. Climate change in the circum-North Atlantic region during the last deglaciation. Nature 338, 553–557.

Peteet, D.M., Vogel, J.S., Nelson, D.E., Southon, J.R., Nickmann, R.J., Heusser, L.E., 1990. Younger Dryas climatic reversal in northeastern USA? AMS ages for an old problem. Quat. Res. 33, 219–230.

Porter, S.C., 1978. Glacier Peak tephra in the North Cascade Range, Washington: stratigraphy, distribution, and relationships to late-glacial events. Quat. Res. 10, 30–41.

Pye, K., 1995. The nature, origin and accumulation of loess. Quat. Sci. Rev. 14, 653–667.

Reasoner, M.A., Osborn, G., Rutter, N.W., 1994. Age of the Crowfoot advance in the Canadian Rocky Mountains: a glacial event coeval with the Younger Dryas oscillation. Geology 22, 439–442.

Reidel, S.P., 1978. The Stratigraphy and Petrogenesis of the Grande Ronde Basalt in the Lower Salmon and Adjacent Snake River Canyon. Ph.D. dissertation, Washington State University, Pullman, WA.

Sea, D.S., Whitlock, C., 1995. Postglacial vegetation and climate of the Cascade Range, central Oregon. Quat. Res. 43, 370–381.

Smith, C.S., 1983. 4300 Year History of Vegetation, Climate, and Fire from Blue Lake, Nez Perce County, Idaho. M.A. thesis, Washington State University, Pullman, WA.

Stevenson, B.A., 1997. Stable Carbon and Oxygen Isotopes in Soils and Paleosols of the Palouse Loess, Eastern Washington State: Modern Relationships and Applications for Paleoclimatic Reconstruction. Ph.D. dissertation, Colorado State University, Fort Collins, CO.

Taylor, K.C., Lamorey, G.W., Doyle, G.A., Alley, R.B., Grootes, P.M., Mayewski, P.A., White, J.W.C., Barlow, L.K., 1993. The 'flickering switch' of late Pleistocene climate change. Nature 361, 432–436.

United States Environmental Data Service, 1968. Climatic Atlas of the United States. US Gov. Printing Office, Washington, DC.

Vallier, T.L., 1974. The Permian and Triassic Seven Devils Group, Western Idaho and Northeastern Oregon. US Geol. Surv. Bull. 1437.

Welhan, J.A., 1987. Stable isotope hydrology. In: Kyser, T.K. (Ed.), Stable Isotope Geochemistry of Low Temperature Processes. Short Course Handbook 13. Mineralogical Association of Canada, Saskatoon, SK, pp. 129–157.

Wentworth, C.K., 1922. A scale of grade and class terms for clastic sediments. J. Geol. 30, 377–392.

Western Regional Climate Center, 2000. Idaho Climate Summaries. http://www.wrcc.dri.edu/summary/climsmid.html.